2024 IEEE/RSJ International Conference on Intelligent Robots and Systems (IROS)
October 14-18, 2024. Abu Dhabi, UAE

Reconfigurable Multi-Rotor for High-Precision Physical Interaction

Joshua Taylor[1,2], Nursultan Imanberdiyev[2], Meng Yee (Michael) Chuah[2],
Wei-Yun Yau[2], Guillaume Sartoretti[1], and Efe Camci[2]

***Abstract*— Unmanned aerial vehicles (UAVs) for contact-based tasks at height can greatly improve the safety of the human workers involved. However, performing contact-based tasks with typical under-actuated UAVs is non-trivial. Due to their coupled translational and rotational dynamics and their limited station-keeping performance under physical disturbances, it is difficult to maintain precise and consistent contact. We address these problems in the context of physical interaction with vertical, cylindrical target objects, such as trees. We present a novel UAV design with a pair of tilt-rotors and a landing gear that can reconfigure into a front-mounted, two-fingered gripper. While the tilt-rotors provide horizontal force toward the target object without pitching the UAV forward, the reconfigurable landing gear enables the UAV to obtain support from the target object. Such support results in an approximately 80% improvement in position- and heading-keeping performance. Moreover, the landing gear is designed as a cable-driven under-actuated system, which requires only one actuator to control both the reconfiguration and the grasping (i.e., five degrees of freedom in total). Such a minimalist design helps keep the UAV power consumption for interactions low. This marks progress towards safe, high-precision physical interaction against vertical, cylindrical target objects. Our UAV in action: https://youtu.be/D-65vldox_A.**

I. Introduction

Unmanned aerial vehicles (UAVs) are unmatched in their ability to operate in hard-to-reach places at high altitudes. This has resulted in their use across many applications, from search and rescue [1] to nature conservation [2]. Most of these applications involve simple surveillance tasks where the UAV can maintain safe distances from any obstacles. More recently, there has been a drive to reap the benefits of UAVs in applications involving physical interaction with the environment. For example, UAVs have been used for aerial screwing and drilling [3], contact-based inspection of power lines [4], and sensor placement on trees [5]. These tasks are typically conducted by human workers, which often require them to reach dangerous locations. Providing UAVs that can handle these tasks has significant implications for worker safety and the amount of resources required.

However, transitioning from vision-based to contact-based tasks is non-trivial for UAVs [6]–[8]. Many applications require accurate initial contact at a specific position, e.g., to mate with a previously placed bolt for unscrewing. Moreover, during physical interaction, deviation from a pose setpoint can lead to high levels of stress on the end effector. These factors present the need for high positional accuracy prior to and during interaction. Such accuracy is difficult to achieve due to the under-actuation of typical rotary-wing UAVs, i.e., they have fewer actuators than degrees of freedom (DoFs), and their translational and rotational dynamics are coupled. Furthermore, the wall effect starts to occur while flying very close to a target object and acts as a disturbance. All these make it difficult to control the UAV precisely and maintain accurate contact with external objects.

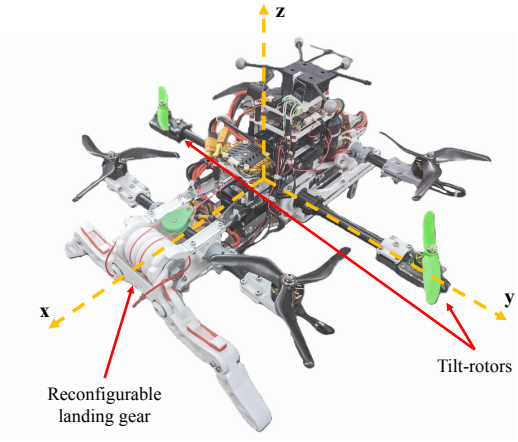

Fig. 1. Novel UAV prototype for high-precision physical interaction.

One approach used in the literature to mitigate these issues is adding further DoFs to the manipulator so that it can move relative to the UAV's body [9], [10]. This alleviates the need for high positional accuracy of the UAV because the manipulator can reach the target location even though the UAV is not perfectly positioned. Alternatively, the manipulator can also be rigidly fixed to the UAV's body when fully-actuated or over-actuated UAVs are used [6]–[8], [11]. Such UAV designs have a number of actuators equal to or greater than the number of DoFs, respectively, which allow them to translate without pitching and rolling, and hover at any arbitrary angle. However, this comes at the cost of additional actuators; therefore, researchers have also explored minimal configurations to obtain only the required benefit. For example, by mounting a single horizontal thruster, the UAV in [12] can generate forward thrust without pitching.

To further improve a UAV's stability during interaction and allow for the generation of larger forces, one can also explore using the target object as support via perching mechanisms. The key challenge here is keeping the design lightweight, hence the adoption of under-actuated cable-driven mechanisms [13], [14], bi-stable mechanisms [15], and reconfigurable UAV bodies [16], which typically allow for fewer added actuators and components. The most

[1]National University of Singapore (NUS), Singapore.
[2]Institute for Infocomm Research (I^{2}R), A*STAR, Singapore.

common approach for perching on vertical surfaces is using suction-based mechanisms [3], [17], [18]. While this method performs well in urban environments with smooth concrete target surfaces, it does not translate well to rougher surfaces like tree bark. Furthermore, several such perching mechanisms are mounted to under-actuated UAVs and, therefore, require agile maneuvers for landing on vertical or near-vertical surfaces [18]–[20]. This may not be suitable for heavy UAVs with high payloads.

In this paper, we present a novel multi-rotor platform for precise contact-based applications against vertical, cylindrical target objects, such as trees and poles. The UAV has a pair of variable tilt-rotors for generating horizontal thrust and a landing gear that can reconfigure into a front-mounted gripper for stabilizing the UAV against the target object. These components require the addition of only two actuators to the UAV, resulting in an overall lightweight design. Through real-world experiments involving interaction with a tree-like target, we show that these capabilities enable the generation of an independent forward thrust while achieving significantly improved position and yaw control. This is key in enabling more stable and safer interactions of the UAV with the environment. Importantly, our system is not limited to smooth vertical surfaces and avoids requiring agile maneuvers to make contact. In summary, the key contributions of this work are:

- A novel UAV design with two tilt-rotors and a landing gear that can be reconfigured as a gripper.
- Design of such lightweight and versatile landing gear which requires only one servo motor for actuation.
- Improved position and yaw control during physical interaction for safer high-precision applications against vertical surfaces of cylindrical objects.

The remainder of this paper is structured as follows. Section II describes the proposed UAV, Section III discusses its control, and Section IV describes the experiments conducted. Finally, Section V describes the current system's limitations, and Section VI draws the key conclusions.

II. The UAV

The UAV concept is shown in Fig. 1. It has four primary thrust rotors arranged in a 260 mm×260 mm square, and two smaller tilt-rotors longitudinally centered and laterally 200 mm apart from the center line. The UAV has a landing gear that can reconfigure into a gripper, henceforth referred to as the *reconfigurable landing gear* (RLG).

A. Tilt-Rotors

To enable the UAV to generate a forward or backward force without pitching, we add a pair of tilt-rotors. This serves as a minimal configuration to decouple pitch and longitudinal motion. This ability allows for a more controlled and precise motion when approaching a target object, which can be particularly useful in confined spaces. Furthermore, it can aid in generating supportive forces for contact-based work, such as a feed-force for drilling. The mechanism used to tilt the rotors is shown in Fig. 2. The two rotors are fixed to one arm, which runs through the center of the UAV body. This arm is rotated via a 1:1 gear train powered by an off-axis servo motor. Rotation of the arm allows for simultaneous tilting of the rotors about the UAV's y-axis.

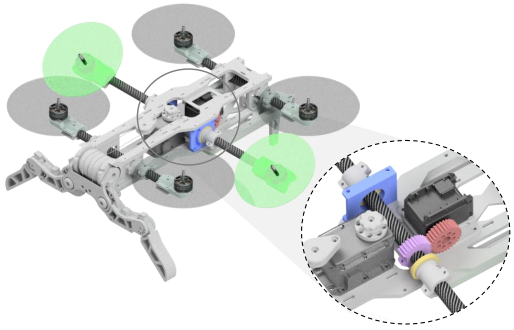

Fig. 2. The tilt-rotor mechanism, consisting of two rotors (green), which rotate simultaneously about the arm's central axis. A gear (red) is fixed to a servo motor head, which drives a gear (purple) on the rotor arm. The arm rotates via bearings (yellow), which fit within a custom housing (blue).

B. Reconfigurable Landing Gear

The key novelty of the UAV is the RLG, which can be raised for use as a gripper, as shown in Fig. 3. This enables grasping onto the target object such that the UAV can rigidly fix itself in place, allowing for the opposition of a wider range of forces and improved station-keeping during interaction. We designed a reconfigurable system to minimize the UAV's weight, as it removes the need for an independent gripper and a landing gear. Such reconfigurability also improves the UAV's weight distribution during regular flights. Lowering the RLG when it is not used for grasping shifts the center of mass toward the aerodynamic center of the UAV. Compared to a UAV that flies with a forward-extended gripper, this induces less stress on the front motors, leading to better stability, energy efficiency, and easier controller tuning.

The RLG has five DoFs (i.e., two joints per finger and one for reconfiguration). Instead of independently actuating each joint, they are all coupled via an under-actuated, cable-driven system, which requires only one servo motor for actuation. This yields a lighter system and enables the use of a pulley differential to allow the gripper to conform to the target surface. It also allows the servo motor to be placed near the center of the UAV for better weight distribution. Figure 3 depicts the system in its key positions. The RLG is passively drawn into the landing gear position in Fig. 3a using elastic cables at the joints. To transition through the remaining positions, the RLG is designed as a series of mechanisms operated by winding in an inelastic cable about the servo drum. The mechanisms are operated sequentially by locking the joints at certain positions via the part geometry. In the landing gear position shown, locking the base link about the fixed RLG mount is achieved using a disc on the proximal link coupled with a recess in the RLG mount. When grounded, the elastic components, as well as the weight of the UAV, draw the disc into the recess, which acts as a key to prevent the rotation so that the landing gear does not collapse outwards. Once the UAV is in the air, winding in the cable releases this lock, allowing this rotation to occur.

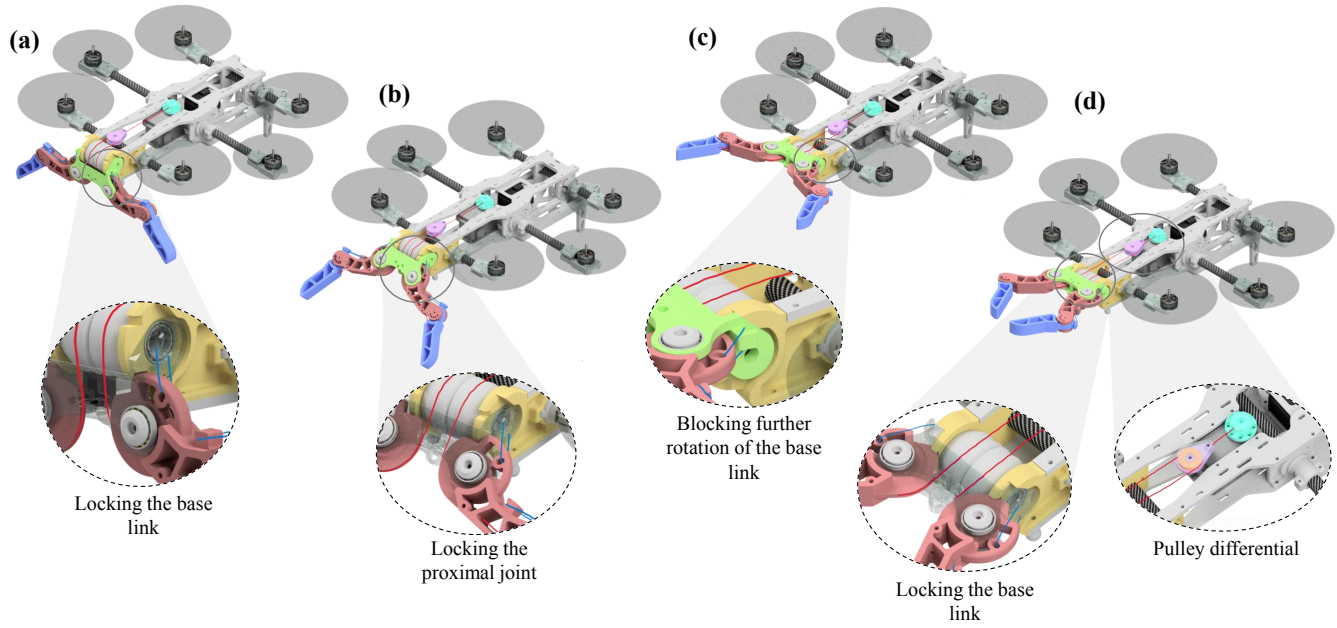

Fig. 3. **The reconfigurable landing gear**, made up of the cable drum (light blue), the pulley differential casing (purple) and the pulley (orange), the RLG mount (yellow), the base link (green), the proximal links (red), and the distal links (dark blue). The inelastic cables (red) and elastic cables (blue) are also depicted. The key positions of the RLG include the **(a)** landing gear position, **(b)** RLG being raised, **(c)** RLG raised and open, and **(d)** closed gripper. Note that the base link (green) is transparent for clarity in certain close-ups.

As it is being raised, as shown in Fig. 3b, rotation of the proximal link is blocked by the RLG mount, ensuring the gripper cannot close until it is completely raised. Rotation of the distal link in this position is prevented by ensuring the joint has a higher rotational stiffness, such that the force needed to rotate is higher than that needed to raise the RLG. The RLG mount blocks the base link once it reaches the upright position, as shown in Fig. 3c. Closure of the RLG is then shown in Fig. 3d, where the disk on the proximal link can now pass through a slot in the RLG mount. This also provides a lock against the rotation of the base link for improved rigidity. The system acts as an under-actuated gripper in this position, like those in [21]. A pulley differential enables the gripper's joints to rotate at differing rates as the cable is wound up, allowing the gripper to conform to the target. Finally, the elastic cables return the RLG to its initial state as the inelastic cable is unwound.

C. Prototype

All structural components were 3D-printed in polylactic acid (PLA) filament, laser-cut from acrylic sheets, or cut from carbon-fiber tubes. We used 1 mm diameter fishing line for the inelastic cable, rubber bands for the elastic components, thin foam for the contact surface of the proximal and distal links of the RLG, and an assortment of steel and nylon fasteners. The electrical components are shown in Fig. 4. The resulting UAV weighs 2.37 kg, with approximately 25% of the mass belonging to the tilt-rotor and RLG components.

III. Control

The following subsections describe the control of the UAV. The control plugins for the tilt-rotors and the RLG were incorporated into the PX4 firmware [22] running on the Pixhawk 4 flight controller.

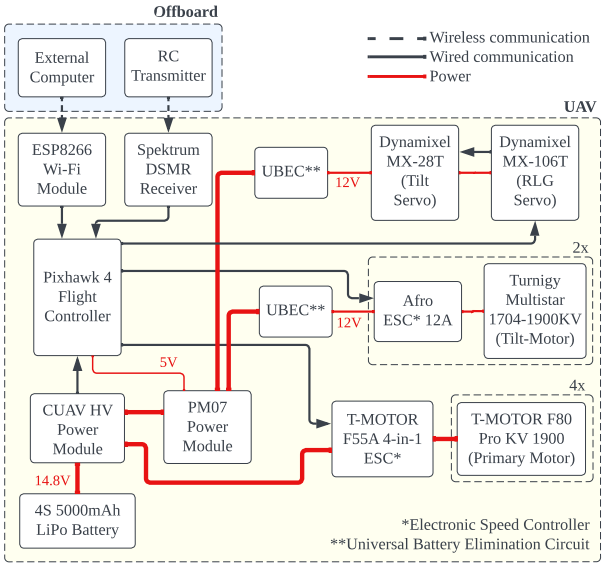

Fig. 4. The electronics architecture implemented for the UAV, including onboard and offboard components.

A. Flight Control

We use an offboard position controller in the Robot Operating System (ROS) paired with the onboard lower-level PX4 controllers. This includes the default PX4 quadcopter mixer for control allocation for the primary rotors. During regular flights, the UAV pitches to travel forward and backward, and the tilt-rotors are kept in the vertical position, providing thrust in the body z-axis.

Once pitching is disabled via the RC transmitter, the tilt-rotors start tilting, providing longitudinal force to travel forward and backward. Position in the y and z body frame

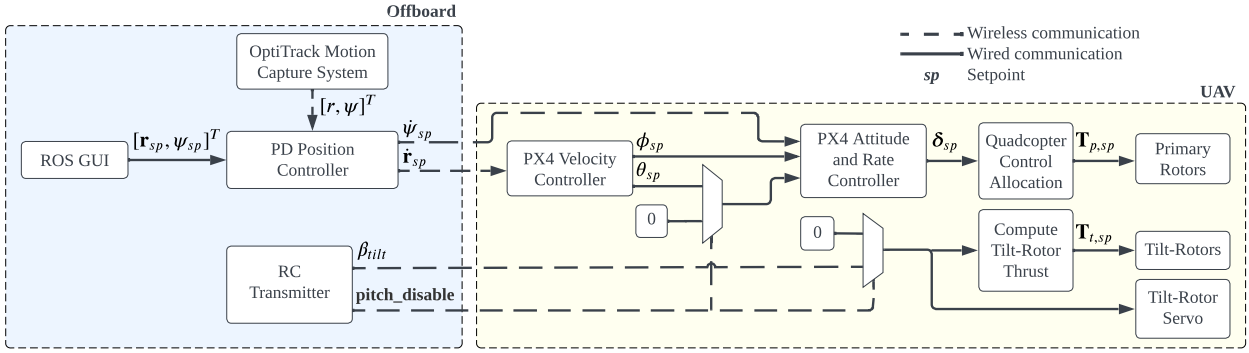

Fig. 5. The control architecture used to operate the UAV. We integrate our system into the existing PX4 control framework [22].

axes are still controlled by the primary rotors. The tilt-angle is directly mapped to the RC transmitter pitch stick, where the maximum point on the pitch stick corresponds to the maximum tilt-angle. This enables an assisted manual flight mode where the UAV operator can maintain some control over the interaction during, for example, inspection or drilling. In this mode, the thrust generated by each tilt-rotor is adjusted according to the tilt-angle to maintain a constant upward thrust, minimizing the disturbance imparted along the z-axis, as per:

$$T_t = \frac{T_{t,u}}{cos(\beta_{tilt})} \tag{1}$$

where T_t is the thrust generated by each tilt-rotor, $T_{t,u}$ is the thrust generated when in the upright position, and β_{tilt} is the tilt-angle from the vertical. Note that a limit of ±45° is imposed on the tilt-angle to avoid saturating the tilt-rotors, and the two tilt-rotors spin in opposite directions to minimize their effect on the UAV's yaw control.

The architecture is depicted in Fig. 5. The position vector is $r = [x \quad y \quad z]^T$, and the attitude vector is defined as $\Psi = [\phi \quad \theta \quad \psi]^T$, which corresponds to roll, pitch, and yaw, respectively. The switch, $pitch\_disable$, defines whether pitching or the tilt-rotors are used to generate longitudinal forces. The torque and scalar thrust commands are given by $\boldsymbol{\delta} = [\delta_{\tau_x} \quad \delta_{\tau_y} \quad \delta_{\tau_z} \quad \delta_T]^T$, and the thrust commands for the primary rotors and tilt-rotors are given as $\mathbf{T}_p = [T_1 \quad T_2 \quad T_3 \quad T_4]^T$ and $\mathbf{T}_t = [T_5 \quad T_6]^T$, respectively. The input to the PX4 attitude and rate controller is a quaternion setpoint; however, Euler angles are shown for simplicity. We obtain position feedback using an external motion capture (MoCap) system.

B. Reconfigurable Landing Gear Control

The RLG is controlled by defining three positions of the Dynamixel MX-106T servo motor, which operates in continuous mode. Each position corresponds to one of the following states: landing gear position (Fig. 3a), gripper raised and open (Fig. 3c), and gripper raised and closed[1] (Fig. 3d). The desired state is commanded through the RC transmitter during flight.

[1]Note that this final position must be tuned for current testing purposes to fit the size of the tree being grasped.

IV. Testing

We conducted several real-world experiments to assess the UAV's performance, including free-flight and physical interaction tests. These are outlined in the following subsections.

A. Independent forward thrust

We verify the UAV's ability to generate an independent forward thrust without pitching. We conduct two flights with forward motion: an under-actuated flight where pitching is used, and a flight where only thrust vectoring by tilt-rotors is used. In both flights, the UAV travels 1 m forward from its initial position. The forward speed is similar across the two tests, albeit slightly varied due to the assisted manual flight mode during the tilt-rotor flight. The results are shown in Fig. 6. Compared to under-actuated flight, the UAV could travel forward with a reduced change in pitch angle when tilt-rotor flight is enabled.

B. Interaction

Next, we test the UAV's ability to achieve high position accuracy during physical interaction. We perform an ablation study to identify the effects of the tilt-rotors and the RLG on the UAV's performance. This includes the following tests:

1) Free-flight: Traditional station-keeping next to the target object without tilt-rotors or RLG, as a baseline.
2) Grasp: Station-keeping while grasping the target object without tilting the rotors.
3) Grasp and push: Station-keeping while grasping the target object and pushing with the tilt-rotors to imitate a typical feed-force task.

The three case studies are depicted in Fig. 7. The target object has a diameter of approximately 210 mm, which cannot be fully grasped by the RLG. The object is 3D-printed from PLA, with a textured surface to mimic tree bark. We conduct batched tests to mitigate the stochasticity effect, which is inevitable in real-world systems. We repeat each of the three case studies five times. Each repetition starts with a fully charged battery and lasts for 10 seconds. We benchmark our UAV's performance based on position- and heading-keeping as well as power consumption.

Figure 8 depicts the UAV's deviation from the initial position (as the Euclidean norm) and the initial heading over one

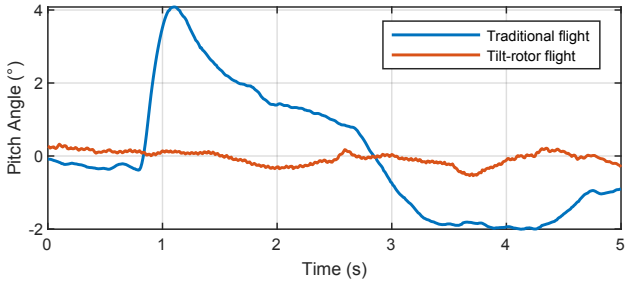

Fig. 6. Orientation data during flight from $x = 0$ to $x = 1\,\text{m}$ to verify the UAV's ability to generate an independent forward thrust.

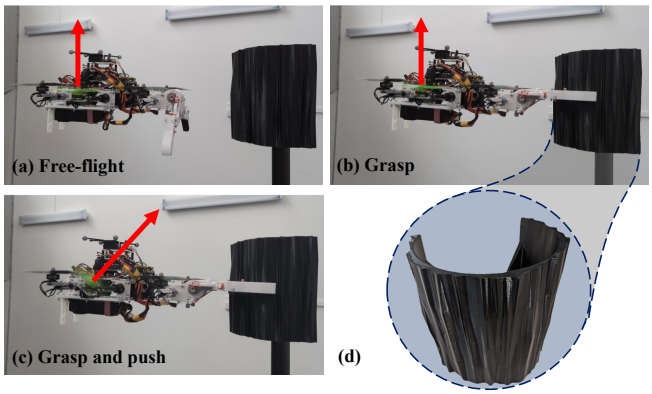

Fig. 7. The case studies for assessing the performance of the RLG and the tilt-rotors. **(a)** Traditional station-keeping. **(b)** Adding the use of the RLG. **(c)** Further adding the use of the tilt-rotors to imitate a feed-force task, creating disturbance. The red arrows depict the direction of tilt-rotor thrust. **(d)** The 3D-printed target object used for testing has a rough outer surface designed to mimic tree bark.

iteration from each case study. The UAV's free-flight station-keeping performance is limited; however, grasping the target object with the RLG significantly reduces position and yaw deviation. These improvements appear slightly offset by the tilt-rotors, yet the effect of this disturbance is minimal.

In applications like drilling, the maximum deviation from the initial point is an important metric that affects the highest stress applied to the end-effector. In Table I, we provide the maximum deviation experienced by the UAV across any of the five iterations for each case study. Furthermore, Table II shows the mean and range of average deviations for each case study's five iterations. In terms of both maximum and average deviation, grasping provides a 90% improvement in position—and heading-keeping performance compared to free flight. When tilt-rotor disturbance is introduced, such improvement remains at around 80%.

In terms of extra power consumption needed during physical interaction tasks, the use of RLG and tilt-rotors causes only a slight increase in power consumption. Table II shows the mean and range of the UAV's average power consumption across each case study's iterations, recorded by the CUAV HV power module. Overall, the use of RLG and tilt-rotors amounts to just a 7% increase in power consumption compared to free-flight. However, it is important to note that during free-flight, the UAV carries the tilt-rotors and RLG without activating them. Hence, the free-flight power consumption value is likely inflated.

TABLE I

MAXIMUM POSITION NORM & YAW DEVIATION EXPERIENCED BY THE UAV ACROSS ANY ITERATIONS FOR EACH CASE STUDY.

	Position Norm (m)	Yaw (°)
Free-flight	0.083	8.8
Grasp	0.010	0.8
Grasp and push	0.016	1.4

TABLE II

MEAN POSITION NORM & YAW DEVIATION AND POWER CONSUMPTION VALUES FOR EACH CASE STUDY, AVERAGED OVER FIVE ITERATIONS.

	Position (m)		Yaw (°)		Power (W)	
	Mean	Range	Mean	Range	Mean	Range
Free-flight	0.032	0.022	2.4	3.4	815	24
Grasp	0.004	0.003	0.2	0.3	828	97
Grasp and push	0.007	0.005	0.4	0.7	869	82

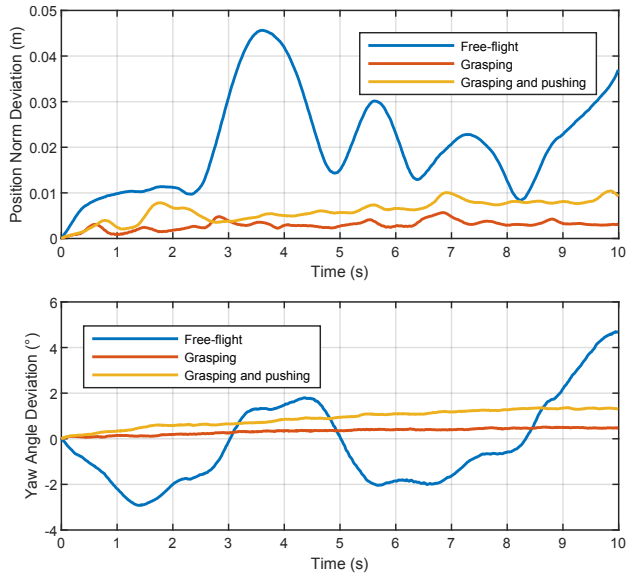

Fig. 8. Deviation from the initial position (top) and heading (bottom) during 10 seconds of interaction. We report the ground truth data from the MoCap system. The test iterations shown here are the best for each case study in terms of maximum position norm deviation.

V. LIMITATIONS

Despite demonstrating performance gains, the current system has limitations. First, by hard-coding the RLG positions, we are not using the RLG's ability to conform to the target's size and shape. In future work, we will use servo motor feedback (e.g., current drawn) to define when the gripper should stop closing. While this should allow for an improved grasp, it may also affect the UAV's power consumption.

There are also limitations on the UAV's flight control. Firstly, MoCap is used for state estimation during our experiments, which does not translate to real-world environments. We will explore methods such as visual servoing to approach the target, to reduce reliance on accurate state estimation. Furthermore, during interaction, the UAV maintains its position where the grasp is initiated. This position may not be aligned with the current position setpoint due to the UAV's limited free-flight position control performance. Since the

setpoint is static, the controller may attempt to oppose the support from the RLG. Visual servoing would rectify this problem to some extent by eliminating the use of a global setpoint. However, we will also explore more interaction-friendly control schemes, such as admittance control [23].

VI. Conclusion

In this work, we presented a novel UAV design with a pair of tilt-rotors and a reconfigurable landing gear (RLG). The tilt-rotors enable the UAV to generate an independent forward thrust for feed-force tasks, and the RLG enables the UAV to obtain support from the target object. When both mechanisms are activated while flying against a vertical, cylindrical target object with a rough surface, the position- and heading-keeping accuracy of the UAV is improved by approximately 80%. This improvement is measured in terms of maximum and average deviation from an initial position and yaw. This performance comes at the cost of only a 7% increase in average power consumption during interaction.

Our future work will include assessing the size of the independent forces and torques the UAV can generate in response to interaction with the environment and external disturbances such as wind. We will then apply the UAV to real-world, high-precision, contact-based applications. An example includes drilling into trees to detect rot. For such an application, where the target surface may not be perfectly vertical, we will explore using tilt-rotors as the main thrusters to hover at various orientations. We also plan to explore greater autonomy during interaction. This includes using feedback in the RLG's control system to enable adaptive grasping and implementing more interaction-friendly flight control using visual servoing or admittance control schemes.

ACKNOWLEDGMENT

Joshua Taylor is an A*STAR scholar under the Singapore International Graduate Award (SINGA) framework. This research is partially supported by by National Research Foundation, Singapore under Award No CoT-V1-2023-2 and A*STAR C221518004. Lastly, the authors thank Mohammad Asif for his help in running the experiments.

References

[1] Teodor Tomic, Korbinian Schmid, Philipp Lutz, Andreas Domel, Michael Kassecker, Elmar Mair, Iris Lynne Grixa, Felix Ruess, Michael Suppa, and Darius Burschka. Toward a fully autonomous uav: Research platform for indoor and outdoor urban search and rescue. *IEEE robotics & automation magazine*, 19(3):46–56, 2012.

[2] Jan C van Gemert, Camiel R Verschoor, Pascal Mettes, Kitso Epema, Lian Pin Koh, and Serge Wich. Nature conservation drones for automatic localization and counting of animals. In *Computer Vision-ECCV 2014 Workshops: Zurich, Switzerland, September 6-7 and 12, 2014, Proceedings, Part I 13*, pages 255–270. Springer, 2015.

[3] Roman Dautzenberg, Timo Küster, Timon Mathis, Yann Roth, Curdin Steinauer, Gabriel Käppeli, Julian Santen, Alina Arranhado, Friederike Biffar, Till Kötter, et al. A perching and tilting aerial robot for precise and versatile power tool work on vertical walls. In *2023 IEEE/RSJ International Conference on Intelligent Robots and Systems (IROS)*, pages 1094–1101. IEEE, 2023.

[4] Lei Yang, Junfeng Fan, Yanhong Liu, En Li, Jinzhu Peng, and Zize Liang. A review on state-of-the-art power line inspection techniques. *IEEE Transactions on Instrumentation and Measurement*, 69(12):9350–9365, 2020.

[5] Christian Geckeler and Stefano Mintchev. Bistable helical origami gripper for sensor placement on branches. *Advanced Intelligent Systems*, 4(10):2200087, 2022.

[6] Caiwu Ding, Lu Lu, Cong Wang, and Caiwen Ding. Design, sensing, and control of a novel uav platform for aerial drilling and screwing. *IEEE Robotics and Automation Letters*, 6(2):3176–3183, 2021.

[7] Micha Schuster, David Bernstein, Paul Reck, Salua Hamaza, and Michael Beitelschmidt. Automated aerial screwing with a fully actuated aerial manipulator. In *2022 IEEE/RSJ International Conference on Intelligent Robots and Systems (IROS)*, pages 3340–3347. IEEE, 2022.

[8] Pedro Henrique Mendes Souza and Karl Stol. Constrained dynamics of an aerial manipulator interacting with flexible cantilever beams. *IEEE/ASME Transactions on Mechatronics*, 28(2):967–975, 2022.

[9] Jasper LJ Scholten, Matteo Fumagalli, Stefano Stramigioli, and Raffaella Carloni. Interaction control of an uav endowed with a manipulator. In *2013 IEEE International Conference on Robotics and Automation*, pages 4910–4915. IEEE, 2013.

[10] T Bartelds, Alex Capra, Salua Hamaza, Stefano Stramigioli, and Matteo Fumagalli. Compliant aerial manipulators: Toward a new generation of aerial robotic workers. *IEEE Robotics and Automation Letters*, 1(1):477–483, 2016.

[11] Karen Bodie, Maximilian Brunner, Michael Pantic, Stefan Walser, Patrick Pfändler, Ueli Angst, Roland Siegwart, and Juan Nieto. Active interaction force control for contact-based inspection with a fully actuated aerial vehicle. *IEEE Transactions on Robotics*, 37(3):709–722, 2020.

[12] Takamasa Kominami, Zou Liang, Ricardo Rosales Martinez, Hannibal Paul, and Kazuhiro Shimonomura. Physical contact with wall using a multirotor uav equipped with add-on thruster for inspection work. In *2023 IEEE/RSJ International Conference on Intelligent Robots and Systems (IROS)*, pages 6955–6961. IEEE, 2023.

[13] William RT Roderick, Mark R Cutkosky, and David Lentink. Bird-inspired dynamic grasping and perching in arboreal environments. *Science Robotics*, 6(61):eabj7562, 2021.

[14] Andrew McLaren, Zak Fitzgerald, Geng Gao, and Minas Liarokapis. A passive closing, tendon driven, adaptive robot hand for ultra-fast, aerial grasping and perching. In *2019 IEEE/RSJ International Conference on Intelligent Robots and Systems (IROS)*, pages 5602–5607. IEEE, 2019.

[15] HaoTse Hsiao, Jiefeng Sun, Haijie Zhang, and Jianguo Zhao. A mechanically intelligent and passive gripper for aerial perching and grasping. *IEEE/ASME Transactions on Mechatronics*, 27(6):5243–5253, 2022.

[16] Weijia Tao, Karishma Patnaik, Fuchen Chen, Yogesh Kumar, and Wenlong Zhang. Design, characterization and control of a whole-body grasping and perching (whopper) drone. In *2023 IEEE/RSJ International Conference on Intelligent Robots and Systems (IROS)*, pages 1–7. IEEE, 2023.

[17] Jim David Ang, Lester Librado, Carl John Salaan, Jonathan Maglasang, Kristine Sanchez, and Marcelo Ang. Drone with pneumatic-tethered suction-based perching mechanism for high payload application. In *2022 IEEE/RSJ International Conference on Intelligent Robots and Systems (IROS)*, pages 12154–12161. IEEE, 2022.

[18] Han W Wopereis, TD Van Der Molen, TH Post, Stefano Stramigioli, and Matteo Fumagalli. Mechanism for perching on smooth surfaces using aerial impacts. In *2016 IEEE international symposium on safety, security, and rescue robotics (SSRR)*, pages 154–159. IEEE, 2016.

[19] Jeffrey Mao, Stephen Nogar, Christopher M Kroninger, and Giuseppe Loianno. Robust active visual perching with quadrotors on inclined surfaces. *IEEE Transactions on Robotics*, 2023.

[20] Liming Zheng and Salua Hamaza. Albero: Agile landing on branches for environmental robotics operations. *IEEE Robotics and Automation Letters*, 2024.

[21] Raymond Ma and Aaron Dollar. Yale openhand project: Optimizing open-source hand designs for ease of fabrication and adoption. *IEEE Robotics & Automation Magazine*, 24(1):32–40, 2017.

[22] Lorenz Meier, Dominik Honegger, and Marc Pollefeys. Px4: A node-based multithreaded open source robotics framework for deeply embedded platforms. In *2015 IEEE international conference on robotics and automation (ICRA)*, pages 6235–6240. IEEE, 2015.

[23] Federico Augugliaro and Raffaello D'Andrea. Admittance control for physical human-quadrocopter interaction. In *2013 European Control Conference (ECC)*, pages 1805–1810. IEEE, 2013.